Development of a compact scintillator-based high-resolution Compton camera for molecular imaging

A. Kishimoto[a], J. Kataoka[a], A. Koide[a], K. Sueoka[a], Y. Iwamoto[a], T. Taya[a], S. Ohsuka[b]

[a] *Research Institute for Science and Engineering, Waseda University, 3-4-1 Ohkubo, Shinjuku, Tokyo, Japan*
[b] *Central Research Laboratory, Hamamatsu Photonics K. K., 5000 Hirakuchi, Hamakita-ku, Hamamatsu, Shizuoka, Japan*

Abstract

The Compton camera, which shows gamma-ray distribution utilizing the kinematics of Compton scattering, is a promising detector capable of imaging across a wide range of energy. In this study, we aim to construct a small-animal molecular imaging system in a wide energy range by using the Compton camera. We developed a compact medical Compton camera based on a Ce-doped $Gd_3Al_2Ga_3O_{12}$ (Ce:GAGG) scintillator and multi-pixel photon counter (MPPC). A basic performance confirmed that for 662 keV, the typical energy resolution was 7.4 % (FWHM) and the angular resolution was 4.5° (FWHM). We then used the medical Compton camera to conduct imaging experiments based on a 3-D imaging reconstruction algorithm using the multi-angle data acquisition method. The result confirmed that for a ^{137}Cs point source at a distance of 4 cm, the image had a spatial resolution of 3.1 mm (FWHM). Furthermore, we succeeded in producing 3-D multi-color image of different simultaneous energy sources (^{22}Na [511 keV], ^{137}Cs [662 keV], and ^{54}Mn [834 keV]).

Keywords: Compton camera, depth of interaction

1. Introduction

In the field of nuclear medicine and small-animal imaging, instruments capable of visualizing the distribution of radioisotopes have an important role. Single photon emission computed tomography (SPECT) and positron emission tomography (PET) have been widely used to detect cancer and identify other lesions. However, the radioactive tracers suitable for each of the devices are strictly limited in terms of energy; SPECT can image only sources of low-energy gamma rays under 300 keV, and PET can image only coincident gamma rays, such as 511 keV gamma rays, from positron-emitting sources. On the other hand, since the Compton camera operates over large gamma-ray energy range (300∼2000 keV), it can produce images of multiple radionuclides at the same time [1, 2]. In addition, because the Compton camera has in principle a 180°-field of view, 3-D imaging is possible at relatively low detector costs.

The Compton camera utilizes the kinematics of Compton scattering:

$$\cos\theta = 1 - \frac{m_e c^2}{E_2} + \frac{m_e c^2}{E_1 + E_2} \qquad (1)$$

where E_1 denotes the energy of the recoil electron and E_2 denotes the energy of the scattered photon. The direction of an incident gamma ray is calculated by the energy and position information in two detectors scatterer and absorber. In the past, we have developed a scintillator-based handheld Compton camera for environmental measurement in order to identify radiation hotspots after the nuclear disaster in

☆

*Corresponding author
Email address: daphne3h-aya@ruri.waseda.jp (A. Kishimoto)

Table 1: Scintillator configuration of the medical Compton camera.

Parameter	Value
SCATTERER	
Crystal dimensions	0.5 mm × 0.5 mm × 3.0 mm
Array	37 × 37
Layer	2 layer
ABSORBER	
Crystal dimensions	2.0 mm × 2.0 mm × 2.0 mm
Array	11 × 11 × 10
Layer	10 layer
DISTANCE	variable (20.0 ∼ 70.0 mm)

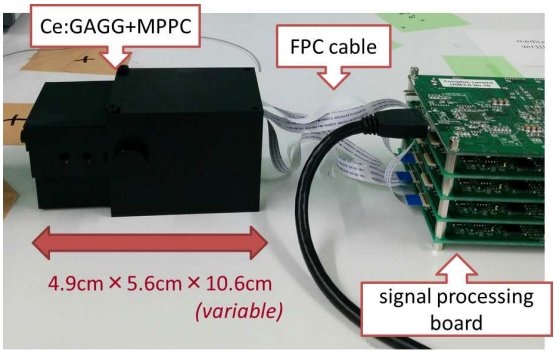

Figure 1: Detector configuration of medical Compton camera.

Fukushima [3, 4]. Although the handheld Compton camera showed high sensitivity, its angular resolution of ∼8° (FWHM) is insufficient for medical use. Now we have been developing a new Compton camera that has both high efficiency and good energy resolution and can be used for medical imaging. In this paper, we report the development of the medical Compton camera and its 3-D imaging results.

2. Development of the medical Compton camera

In developing the medical Compton camera, we used Ce-doped $Gd_3Al_2Ga_3O_{12}$ (Ce:GAGG) scintillator array and 8×8 large monolithic multi-pixel photon counter (MPPC) arrays (Hamamatsu Photonics: S12642-0909-3553(X)) both in the scatterer and the absorber. Table 1 shows the precise configuration of the scintillator block. In order to improve resolution without reducing efficiency, we applied a 3-D position detection method [5] in the absorber.

Fig. 1 shows the configuration of the medical Compton camera. The camera consists of a sensor head and signal processing unit, and the total system weighs only 580 g. The signals from the 4-MPPC arrays go through a resistive charge-division network and a signal processing board, and then they accumulate on a personal computer through a USB 3.0 interface. One of the unique features of the camera is that the resolution, efficiency, and field of view (FOV) can be changed, depending on the measurement situation, by adjusting the distance between the scatterer and the absorber.

3. Basic performance

First we evaluated the resolution of the medical Compton camera. The typical energy resolution for 662 keV became 7.4% (FWHM). Fig. 2 (*left*) shows the angular resolution of the medical Compton camera compared to that of the handheld camera. In this situation, the medical Compton camera had a distance of 50 mm between the scatterer and the absorber. It is clear that the resolution of the medical camera, which had an angular resolution of 4.5° (FWHM) for 662 keV, was significantly better than that of the handheld camera. Fig. 2 (*right*) shows the medical Compton camera-produced image of the ^{137}Cs point source at a distance of 4 cm. We could get the relatively good spatial resolution of 3.1 mm (FWHM). Fig. 3 shows the angular resolution as a function of the distance between the scatterer and the absorber.

The efficiency performance of the medical Compton camera is shown in Fig. 4. It represents the effective count rate when a 1 MBq ^{137}Cs point source is placed at a distance of 30 cm from the camera. As Fig. 3 and Fig. 4 show, resolution and efficiency have a trade-off problem. From here, we made the default distance between the scatterer and the absorber 50 mm in subsequent imaging experiments. The dif-

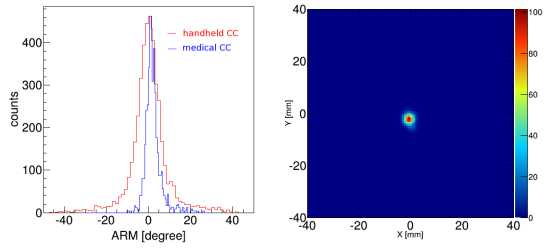

Figure 2: (*Left*) Comparison of angular resolution of handheld and medical Compton cameras, (*right*) imaging result of ^{137}Cs point source measurement using medical CC at a distance of 4 cm.

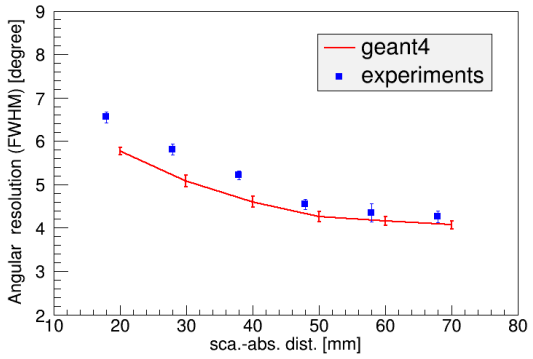

Figure 3: Simulated and experimental angular resolution of the medical Compton camera as a function of the distance between the scatterer and the absorber.

ference between the simulated and experimental results in Fig. 3 and Fig. 4 arises from an incomplete energy calibration of the detectors.

4. Imaging experiments

The goal of our study is to obtain a 3D, multi-color image using the medical Compton camera. For this purpose, we developed a 3-D reconstruction algorithm based on the maximum likelihood expectation maximization (MLEM) method. In general, Compton camera imaging has a large position uncertainty in the depth direction to the camera because of a lack of intersecting data. In order to compensate for this lack of data and get a 3-D isotropic image, we proposed using multi-angle data acquisition method.

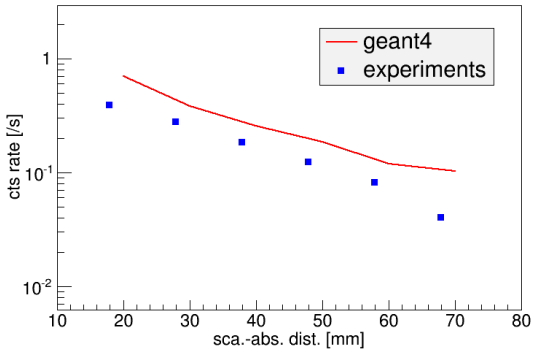

Figure 4: Simulated and experimental efficiency of the medical Compton camera as a function of the distance between the scatterer and the absorber.

Briefly speaking, by measuring the data from several different angles, we can significantly reduce the image uncertainty in the depth direction. Further details are given in ref. [6]. By using the medical Compton camera and the multi-angle data acquisition method, we conducted the following 3-D imaging experiments.

4.1. Phantom imaging

First, we conducted phantom imaging. We used three syringe phantoms filled with a solution of ^{18}F, shown in Fig. 5 (*left*). The diameter of the syringe was 4.5 mm, and the height of the liquid in each syringe was about 10 mm. The distance between the syringes was 15 mm. The total source intensity of the phantom was 0.75 MBq. We applied 12-angle data acquisition (30° pitch), and the total integration time was 15 min. Fig. 5 (*right*) shows the result of 3-D imaging reconstruction by plotting the bins with values over two-thirds of the maximum. The configuration of three syringes was clearly visualized not only 2-dimensionally but also 3-dimensionally.

4.2. Multi-color imaging

Next, we tried to achieve 3-D multi-color imaging. We conducted imaging experiments of three different simultaneous energy sources: ^{22}Na (511 keV), ^{137}Cs (662 keV), and ^{54}Mn (832 keV). Fig. 6 (*a*) shows a diagram of the arrangement of the three energy sources. The distance was 12 mm between ^{22}Na

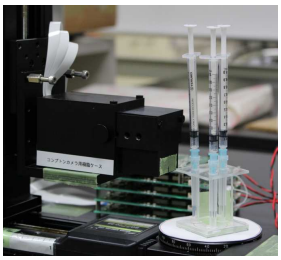

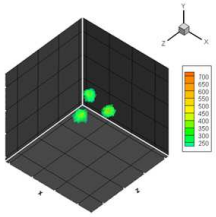

Figure 5: (*Left*) Photograph of syringe phantoms filled with ^{18}F for imaging experiments, (*right*) 3-D reconstructed image based on 12-angle data acquisition.

Table 2: Source configuration in multi-color imaging.

source	energy [keV]	y position [mm]	intensity [MBq]
^{22}Na	511	+12	0.25
^{137}Cs	662	0	0.90
^{54}Mn	834	-9	0.64

and ^{137}Cs and 9 mm between ^{137}Cs and ^{54}Mn. The source configuration is more precisely shown in Table 2. Data was acquired at 12 angles, each taking 30 s. to measure, making 6 min. the total integration time. Fig. 6 (*b*) shows the energy spectrum obtained by summing the energy deposits in the scatterer and the absorber. The three peaks of each source are clearly confirmed, so by applying each energy region of 511 keV, 662 keV, and 834 keV, we can visualize each source. Fig. 6 (*c*) shows the 3-D reconstructed image of the three energy sources, and Fig. 6 (*d*) shows the slice of this image in the y direction. It was found that each source was identified in the correct position. Therefore, we succeeded in obtaining a 3-D multi-color image, or a 3-D image of different energy sources at the same time.

5. Conclusion

In this paper, we reported the development of the Compton camera for medical use and its imaging performance. We confirmed that by using the medical Compton camera and a multi-angle data acquisition method, a 3-D multi-energy image could be obtained

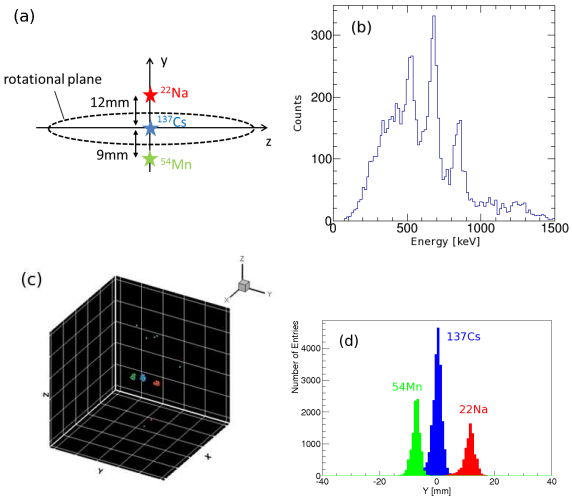

Figure 6: (*a*) Source arrangement for the multi-color imaging experiments, (*b*) Energy spectrum as a sum of detector energy deposits, (*c*) 3-D reconstructed image of ^{22}Na, ^{137}Cs, and ^{54}Mn sources, shown in red, blue, and green, respectively, (*d*) Profile of the image (*c*) in the y direction.

in a relatively short integration time. In the future work, we will try to optimize the reconstruction algorithm and improve the accuracy and speed of the imaging reconstruction. We hope that this study provides significant possibilities for multi-color molecular imaging.

References

[1] S. Enomoto, *Biomed. Res. Trance Elem.*, 16 (2005) 233.

[2] S. Motomura et al., *J. Anual. Atom. Spectrom.*, 28 (2013) 934.

[3] J. Kataoka et al., *Nucl. Instrum. Meth. A*, 732 (2013) 403.

[4] A. Kishimoto et al., *JINST*, 9 (2014) P11025.

[5] A. Kishimoto et al., *IEEE Trans. Nucl. Sci.*, 60 (2013) 38.

[6] A. Kishimoto et al., *JINST*, 10 (2015) P11001.